Design and Control of a Hydraulic Power Take-off for an Axi-symmetric Heaving Point Absorber

Kristof Schlemmer[#1], Franz Fuchshumer[*2], Norbert Böhmer[#3], Ronan Costello[†4], Carlos Villegas[‡5]

[#] *HYDAC System GmbH, Göttelborn, Germany*

[1] kristof.schlemmer@hydac.com

[3] norbert.boehmer@hydac.com

[*] *HYDAC Electronic GmbH, Gersweiler, Germany*

[2] franz.fuchshumer@hydac.com

[†] *National University of Ireland Maynooth, Maynooth, Ireland*

[4] ronan.costello@eeng.nuim.ie

[‡] *Wavebob Ltd., Maynooth, Ireland*

[5] carlos.villegas@wavebob.com

***Abstract*— The FP7 'STANDPOINT' project aims to accelerate the establishment of a standard approach to harvesting energy from the ocean waves by proving that the axi-symmetric, self-reacting point absorber device is a viable technology. In this context, designing a reliable hydraulic power take-off (PTO) system that combines the two apparently contradicting objectives of survivability under extreme weather conditions and efficient, continuous power production is a key challenge. Hence, a hydraulic PTO system is proposed which provides means of energy storage and smoothing to decouple power output and input. A flexible circuit design allows for the implementation of an appropriate damping characteristic and control law that adapt to the sea conditions, and thus enables high efficiency of the energy conversion. Maintainability and adaptability are fostered by the modularity of the hydraulic design. Through optimisation of component layout and sizing, an appropriate compromise is found between installation space and costs on one side and the capability of harvesting power peaks on the other side. For this purpose, a combined dynamic model of the wave energy converter (WEC) system has been developed and simulated for the sea conditions of the Portuguese test site. Simulation results have validated the viability of the hydraulic PTO design.**

***Keywords*— wave energy converter, Wavebob, Hydraulic Parallel Circuit, damping force control, modularity, power adaptation**

I. Introduction

There are major challenges in converting energy from the ocean waves into electricity. Wave energy converters (WEC) not only need to effectively convert the mechanical power into grid compliant electrical power, but also to withstand extreme sea conditions for at least 25 years of operation. There is a perceptible convergence towards floating, off-shore systems that are adapted to oscillate in accordance with the incident wave climate and thus maximise energy absorption. One of such devices is the Wavebob (Fig. 1) of the heaving buoy point absorber type. The Wavebob is composed of two heaving buoys: a torus of 14 m in diameter and a float linked to a submerged tank with a draught of 40 m. It is kept in position using a slack mooring and it is capable of detuning from certain sea conditions by rapidly releasing the water trapped in the tank.

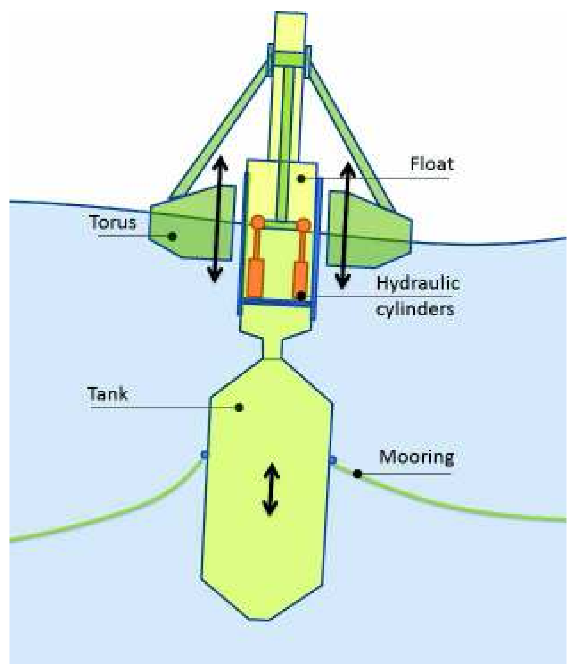

Fig. 1 Wavebob principle of operation

Due to the different mass and hydrodynamic properties, the torus is characterised by a high natural frequency, while the float acts as a high-inertia body with a low natural frequency. When excited by ocean waves, both buoys respond with an oscillation of different amplitudes and phases, thus creating relative motion between them. Since the bodies are connected via a power take-off (PTO) system, the available energy is transformed via the PTO to useful electrical power. In addition, the forces applied by the PTO system provide damping to the relative motion, changing the response of the overall body. For example, if a high damping force is applied, both bodies will tend to oscillate without relative motion as if they were a single body. The ability of the PTO to adapt to the incident wave climate allows for the system to survive extreme sea conditions and increases the power capture as indicated by the instantaneous absorbed mechanical power (damping force times relative velocity). The electrical power produced at the PTO system is sent to shore via subsea cables.

The technical challenges in developing PTO systems for wave energy converters are enormous, as they have to accommodate both power absorption and survival of extreme waves. The development of a PTO is carried out in stages going from computer simulations to full scale PTO test rigs [1]. While a computer simulation of the integrated PTO and wave energy converter is suitable for dimensioning the PTO components (*e.g.* accumulators, cylinders), many situations like faults or hydraulic fluid degradation are difficult to model, and an on-shore test rig is needed to test typical operating conditions [1][2].

PTO systems for point absorbers are generally either hydraulic [1][3] or electrical [4][5][6]. An insightful summary of the different PTO system technologies can be found in [7]. Hydraulic systems have important advantages, such as much higher force to weight ratio, energy storage and the use of proven technology. In addition, hydraulic systems are a suitable PTO solution for the low speeds and high forces inherent to the ocean waves [1]. A typical hydraulic PTO system is composed of (1) a pumping module via hydraulic cylinders, (2) energy storage capabilities via hydraulic accumulators and (3) generation via hydraulic motors connected to electrical generators. As shown by experimental results by Henderson [1], the hydraulic energy storage has an important effect on providing a smooth power output to the grid in spite of the large mechanical power fluctuations due to the irregular nature of ocean waves. The sizing of such accumulators for a simple hydraulic PTO is addressed by Falcão [8]. Utilising these advantages, the Wavebob has already been deployed to generate electricity from the ocean waves off the west coast of Ireland using a hydraulic PTO system.

Wave energy technology is still under development, and various companies have been testing demonstrators at Portugal, Scotland, England, Ireland and the US [9]. With a wide range of competing technologies, there is a need to identify a general set of common parameters to accelerate the adoption of agreed norms followed by the development of rules and guidelines for certification. Such development will become increasingly important with the advent of wave farms where tens or hundreds of wave energy converters operating in arrays will supply electricity to the shore. The 'STANDPOINT' project within the European Community's 7th Framework Programme (FP7) will use the design, deployment and continuous operation of a Wavebob to develop and disseminate such rules and guidelines. In this EU-funded project, the Wavebob developers (Ireland) collaborate with Generg (Portugal; site and grid connection), Germanischer Lloyd (Germany; certification and guidelines), Hydac (Germany; hydraulics), and Vattenfall (Sweden; risk analysis).[1]

In 2007, Wavebob's WEC became the first Irish device to successfully harness energy from the ocean waves. A Wavebob prototype is being designed for the STANDPOINT project to use a hydraulic PTO. Such WEC is intended to be deployed in 2012 off the Portuguese coast for one year. In this paper, a novel hydraulic PTO design for this wave energy converter is proposed. For a given set of PTO requirements identified in Section II, two hydraulic PTO concepts are explored in Section III. The control system used is described in Section IV, followed by simulation results of the smooth power output for a typical Atlantic wave climate in Section V.

II. PTO Requirements

A. Functional Requirements

Compared to wind energy, wave energy resources are characterised by certain differences in power input. While it is in average more predictable and reliable, the instantaneous input power is highly irregular and unpredictable, although current research efforts are aiming to provide wave forecasting of a few seconds [10]. Furthermore, the ratio of maximum wave input power $P_{\max}$ to average wave input power P_{avg} is extremely large.

The main challenge to a WEC power take-off system therefore is to safely endure the maximum input power peaks, and at the same time to reasonably and effectively harvest power at the predominant moderate input power levels. Survivability and good power production performance are paramount objectives to be achieved by the PTO. A systematic risk assessment procedure has been utilised to derive the main functional requirements. These have been related to the following categories.

1) Survivability

The WEC must remain buoyant and on station whilst deployed. The force transmission path must remain structurally intact at all times. Any input power in excess of the absorption capabilities of the WEC needs to be dissipated without danger to the device and any personnel.

2) Power Production Performance

A good performance of the power production implies positive ratings of efficiency, power quality and availability. High efficiency of the energy absorption and conversion by the PTO system shall be guaranteed particularly under long-period excitation as encountered at sea. In spite of the irregular power input with peaks of up to several MW, the power output is required to be regular, constant, and reliable within given tolerances, so as to optimise power delivery to the grid. The desired power production capacity is in the order of several hundred kW. Additionally, availability of the power production must be sufficient to render the WEC operation economically profitable.

---

[1] For further information see www.fp7-standpoint.eu

3) Operation and Maintenance Effort

Like other marine off-shore applications, wave energy converters require a comparatively large operation and maintenance effort due to limited accessibility, strong dependence on weather conditions etc. These increased costs need to be contained and minimised. This includes an evaluation and optimisation of reliability, availability and maintenance issues.

From an endurance point of view, the WEC system and its components must be suitably designed for a 1-year test run, a major maintenance interval of 5 years, and a 25-year life.

4) Safety

Fulfilment of the above requirements must not compromise safety of personnel and machinery at any time during operation and maintenance, on shore or off shore. The safety concept must be failsafe and comply with applicable regulations and best practice.

B. Technical Requirements

The functional requirements discussed in Section A are used to derive the technical requirements to be fulfilled by the design and construction of the PTO system. As a main conclusion, wave energy is to be absorbed through hydraulic damping. The damping force is to be controlled by the PTO in the following way:

- Provide large damping forces to guarantee survival in combination with the mechanical end-stop buffers and device structure
- Provide appropriate damping forces to tune/de-tune the oscillation and maximise power absorption

The maximum mechanical forces to be transmitted in extreme sea states can become enormous. It is essential to separate these forces in such a way that only axial forces along the power producing degrees of freedom are channeled to the PTO, while lateral forces and moments are transmitted to the guidance and anti-yaw systems.

The installed flow and force capacities are to be sized according to the expected mean annual input power and the maximum endurable force. These two objectives are contradictive and cannot be achieved at the same time. Hence, in order to optimise the damping and harvesting effect, the system must be equipped with self-tuning capabilities to make it adaptable to changing sea conditions.

A key factor for constant delivery of electrical power in grid-compliant quality is the decoupling of power output from power input. This requires some concept of storing energy. Power ripples can thus be smoothed, and both positive and negative power peaks can be buffered.

Due to the mechanical design of the WEC unit, the available installation space for the hydraulic PTO skid is limited to 4 m in diameter by 11 m in height,

III. Hydraulic System Design

A. Modular Power Adaptation

The capability to fulfil the requirements of Section II B mainly depends on the damping forces and the relative velocities between torus and float. These in turn govern the main hydraulic variables: pump flow, pump pressure, generation flow, and generation pressure. If the hydraulic circuit is bound to a single set of components, their sizing will invariably restrict the range of reasonable use to extents below the desired ones. As a result, the requirements can never be fulfilled satisfactorily, without compromising on some of the objectives that have been identified before.

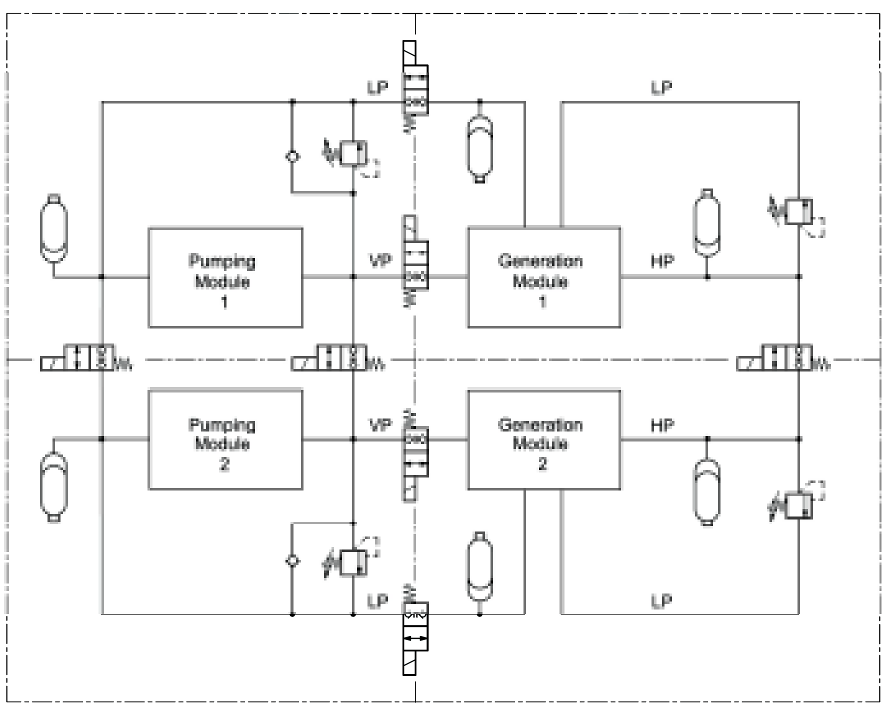

Fig. 2: Modular PTO system schematic

Hence, a power adaptation approach is necessary to solve this problem. The modular hydraulic circuit proposed in Fig. 2 is a way of implementing such an approach. It comprises four sections that can be independently connected or separated through a total of seven leak-proof shut-off valves. Two pumping modules and two generation modules can thus be combined in any desired way, offering a greater variety in the selection of power producing capacity.

The required de-coupling of power output and input is achieved through establishing two separate elevated pressure levels next to the biased low pressure level (LP, 20 bar): variable pressure (VP, 20-250 bar) and high pressure (HP, 250 bar). The HP level is buffered by an accumulator and maintained through HP motor displacement control, providing a nearly constant working pressure for the hydraulic motor by compensating any variations, peaks and ripple. Thus, the excess power of high incident waves is stored for a short period and recuperated at low wave heights. The VP level, on the other hand, is intended to provide a defined backpressure for the pumping module and thus a defined damping force. The key issues here are stiffness and controllability. Any compliance, as in the HP level, therefore is not permissible. The mode that is used to transition from LP to HP via VP is determined by the control law that is described in Section IV.

Additionally, the modular concept is favoured by the reliability, availability, maintainability and safety considerations of Section II A. By sectioning off particular parts of the circuit, failures can be isolated for safe operation, maintenance, and repair. Hydraulic overload protection is provided by pressure relief valves in all VP and HP pressure lines.

B. Power Conversion – Pumping

The incoming oscillating mechanical wave power is converted into hydraulic power at the two cylinders within a pumping module, see Fig. 3. Volumetric flows from both pumping cylinders are joined and build up the variable pressure. The design flow rate thus totals about 2.400 l/min.

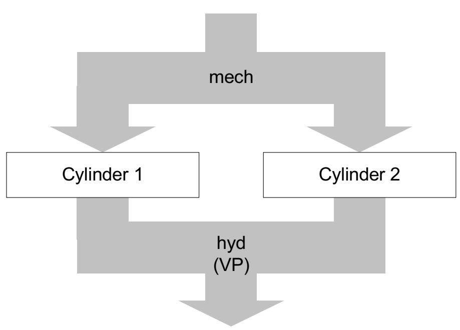

Fig. 3: Power flow and conversion in a pumping module
(mech: mechanical, hyd: hydraulic)

Fig. 4 shows the kinematical set-up of the pumping modules. The cylinders of both modules are arranged in opposite direction and differ in size by a ratio of 2:1, so as to allow for variable combinations of capacity. The cylinders also have an effective area ratio of 2:1. In the valve control manifold, the flow is equalised and rectified such that both extending and retracting strokes yield the same flows and pressures. By opening the pilot-operated inlet check valves in low sea states, a pumping module can be switched to by-pass mode, i.e. no flow is displaced to the VP side. A special guidance system is realised to provide separation of the force transmission paths. In addition to the (de-)tuning capabilities through adaptable venting of the submerged tank, hydraulic cushioning and mechanical end-stop buffers provide additional overload protection and safety to avoid structural damage.

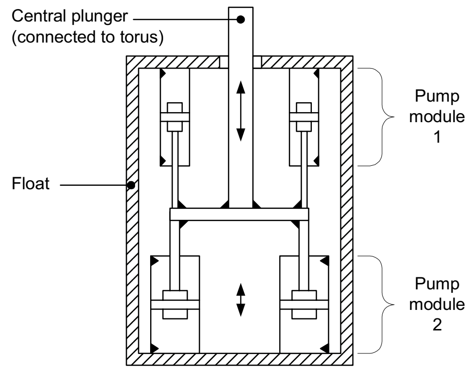

Fig. 4 Cylinder set-up

C. Power Conversion – Generation

In order to deliver electrical power to the grid, the hydraulic power at some point needs to be converted back into mechanical power using hydraulic motors, and finally into electrical power using AC generators. Due to the buffering effect of the hydraulic accumulators, the generation module is designed for a smaller flow rate of about 800 l/min. Two concepts of power transmission and conversion shall be investigated and compared: the Hydraulic Transformer Circuit (HTC) and the Hydraulic Parallel Circuit (HPC). The power flows and conversion steps of these circuits are compared and their hydraulic schematics are illustrated in Fig. 5 through Fig. 8.

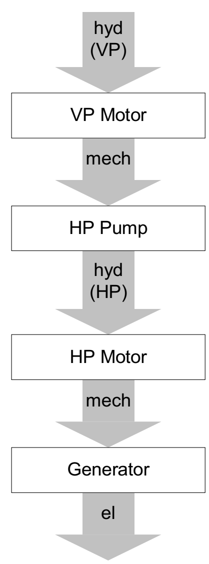

Fig. 5: Power flow and conversion in the Hydraulic Transformer Circuit
(mech: mechanical, hyd: hydraulic, el: electrical)

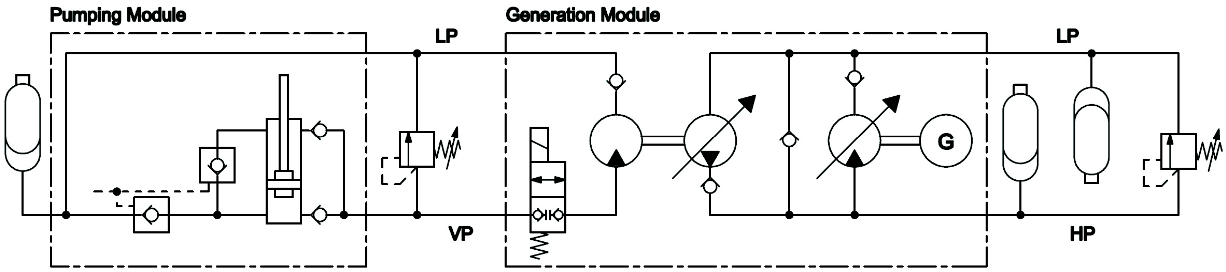

Fig. 6: Hydraulic schematic of the Hydraulic Transformer Circuit (HTC)

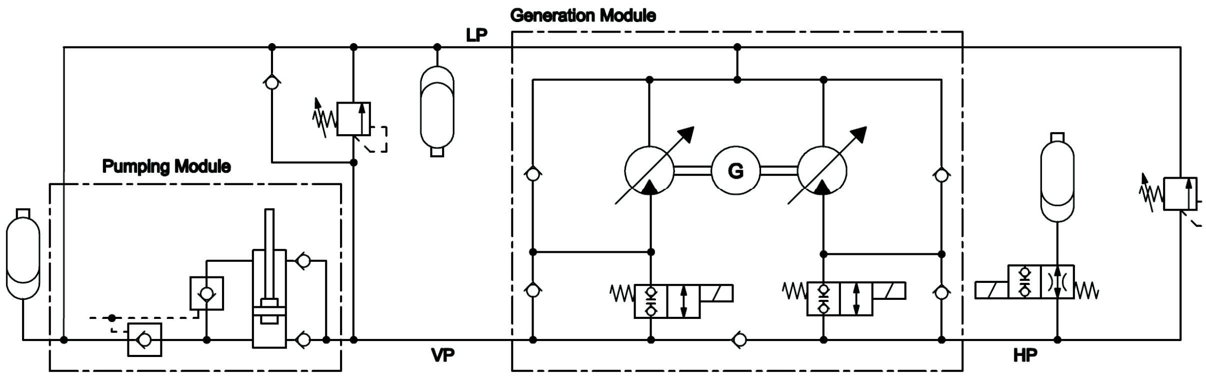

Fig. 7: Hydraulic schematic of the Hydraulic Parallel Circuit (HPC)

The HTC follows a sequential serial approach in terms of power conversion. The generation module mainly consists of a hydraulic transformer, i. e. a device transforming the wave-dependent variable input pressures and flow rates into different output pressures and flow rates at constant theoretical power throughput. This method of de-coupling is achieved by converting the hydraulic input power at a fixed displacement motor into mechanical rotary power. The motor shaft drives a variable displacement pump that converts the mechanical power again into hydraulic power at an arbitrary high pressure level. Buffered by an accumulator, this pressure is utilised to drive a variable displacement hydraulic motor to convert the power back into mechanical power. Finally, it is converted by an AC generator on the same shaft into electrical power.

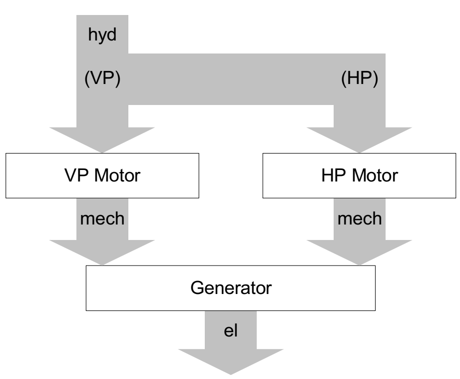

Fig. 8: Power flow and conversion in the Hydraulic Parallel Circuit (mech: mechanical, hyd: hydraulic, el: electrical)

The power generation is completely decoupled from the input by using two separate hydraulic circuits. Thus, the HTC is characterised by great versatility and freely adjustable control in different sea states without any undesired feedback. However, the primary side needs to be sized to account for the maximum input power, which implies a very large hydraulic motor. This means that power peaks can be harvested fairly well, but for average moderate-power input, the units are considerably oversized. As a result, the overall conversion efficiencies are limited, which is aggravated by the fact that the power flow goes through four serial conversion steps in the generation module alone, see Fig. 5. Furthermore, the hydraulic motor/pump unit is operated intermittently, with frequent standstills, low-pressure start-ups and operation in the mixed friction regime negatively affecting component life.

The HPC concept differs from the HTC concept in some essential features. Firstly, the VP and HP levels are not hydraulically de-coupled. There is only a single hydraulic circuit, separated by a check valve that allows passing of excess flow from VP to HP. The AC generator is driven by two variable displacement motors placed in parallel on a common shaft. Thus, both VP and HP sides can be used simultaneously to generate electrical power. While the VP motor displacement is ramping up and down with the wave-dependent input flow, the HP motor is used to maintain a constant generator speed. In higher sea states, the motor is driven directly at full displacement by input flow entering the HP side. Excess flow is used to charge the HP accumulator, or finally throttled off at the pressure relief valve. In low sea states, the check valve remains closed, and the HP motor is driven at reduced displacement by the compressed oil volume stored in the accumulator. Constant pressure and speed conditions can be maintained within the limits set by the accumulator capacity through varying the motor displacement and hence torque and power. The lowest continuously operable sea state is thus a matter of tuning the design to the local wave climate. The control strategy that is used to control the VP and HP pressure levels via the VP and HP motor displacements is discussed in Section IV.

Comparing the corresponding power flow diagrams of HTC and HPC, it becomes clear that the HPC has an essential advantage, since due to its structure it only comprises two sequential power conversion steps, passing only one rotary displacement unit. Additionally, the components of the HPC can be sized with respect to the average expected wave input power, increasing the overall mean efficiency. The maximum harvestable power is determined by the sizes of the HP motor and the HP accumulator: a larger motor allows for greater direct power conversion, while a larger accumulator allows for longer storage periods with delayed power conversion. Apart from longer periods of calm and low seas, standstills of the rotary units are largely avoided in the HPC. It is, however, less flexible than the HTC in terms of realisable control laws. The reason is that it has fewer degrees of freedom and is thus restricted physically to certain damping force characteristics.

The two PTO concepts proposed above are preferable to a direct hydraulic transmission without de-coupling due to more appropriate sizing and smoothing. Furthermore, both HTC and HPC enable stiff damping force control and elastic power smoothing at the same time, while a circuit using only HP and LP levels, such as adopted in [8], can only deliver one of these advantages simultaneously. The comparison and evaluation of the two proposed hydraulic PTO circuits according to Table I yields that the HPC concept is superior to the HTC in most of the relevant criteria. It is therefore selected for continuation of the investigation.

TABLE I
COMPARISON OF HYDRAULIC GENERATION CONCEPTS

Criteria	**HTC**	**HPC**
Power flow	⊖ 4 conversions	⊕ 2 conversions
Hydraulic efficiency	⊙ oversized VP motor	⊕ suitably sized components
Component costs	⊖ additional large components (rotary machine, accumulators…)	⊕ 2-shaft generator
Component life	⊖ intermittent operation	⊕ continuous operation
Damping force control	⊕ fully flexible	⊙ flexible with constraints

IV. DAMPING FORCE CONTROL

Referring to section II B, the main requirements on the damping force control are (i) to produce energy at high efficiency and (ii) to ensure a stable motion between the torus and float and to prevent hitting the end stops of the cylinders. This raises the question of the best damping strategy, see e.g. [8], [11], [12] for some exemplary approaches. By means of numerical analysis, it has been argued in [8] that the energy captured by the wave energy converter is only slightly reduced by using a highly non-linear PTO control law instead of an optimally controlled fully linear one.

But aside from the optimal energy extraction from the waves, it is also important to run the hydraulic circuit in an optimal region in terms of efficiency and lifetime. From the efficiency point of view of the hydraulic PTO system, it is necessary to avoid the low-pressure and part-load regions and instead operate the hydraulic motors close to their maximum displacement and their nominal operating pressure.

As a matter of fact, the power extracted from the waves is oscillating. Therefore, the damping force control has to be designed such that the oscillating power from the waves can be averaged by means of the hydraulic accumulators. On the other hand, it is not always possible to directly transfer the wave energy to the hydraulic accumulators because the pressure corresponding to the desired damping force is lower than the accumulator pressure. In this case, the VP motor is used. At this point, it is important to note that due to the modularity of the hydraulic circuit, three different force levels can be attained at a particular accumulator pressure level, depending on the active pumping modules: (i) pumping module 1 is active, (ii) pumping module 2 is active, (iii) both pumping modules 1 and 2 are active. Considering the aforementioned, the following damping strategy is proposed.

A. Damping Strategy

As illustrated in Fig. 9, the damping strategy comprises two phases: phase 1 with damping force proportional to the relative velocity between the torus and float and phase 2 with nearly constant damping force, where the damping force depends on the accumulator pressure and the pumping modules in use. This mainly corresponds to the so-called latching control, see e.g. [13][14]. Phase 1 is used in calm sea conditions. In this operating phase there is no possibility to store energy by charging the HP accumulator. Phase 2 is used under normal sea conditions. A third phase can be identified, but is generally avoided and thus is not considered part of the damping strategy. This phase is entered, when the HP accumulator either is at its charge limit or is shut off via the shut-off valve. After an elevation of the HP level, the pressure relief valve opens and the excess flow is throttled off to tank. High pressure will then remain nearly constant at the set cracking pressure of the relief valve.

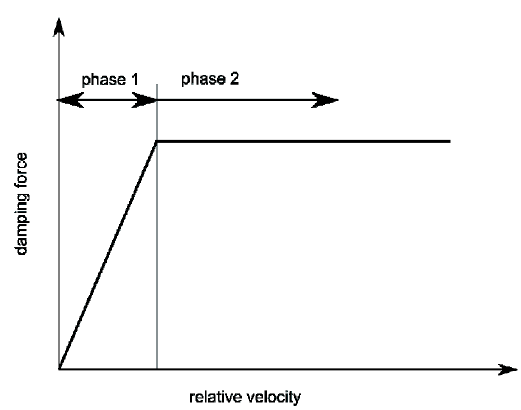

Fig. 9 Damping force characteristic

B. Control Task

The control strategy is based on two levels, (i) the top level control which decides on the usage of the pumping and generation modules and (ii) the low level control which realises the desired damping force and the generation strategy set by the top level control. The requirements on the top level control are mainly the forecast of the sea state in order to decide on the switching of pumping and generation modules as well as the calculation of the desired damping force. The function of the low level control is the realisation of the desired damping force, accumulator pressure and generator power by controlling the VP and HP hydraulic motor displacements.

Based on the required functionality, the control task can be split into two different tasks, (1) the VP motor control and (2) the HP motor control.

(1) Control of the VP motor: this is used to control the desired damping force and pressure of phase 1, respectively, see Fig. 9. In phase 2, the VP motor is run at maximum displacement.

(2) Control of the HP motor: the HP motor displacement acts as a manipulated variable for controlling the HP motor flow rate and thus the accumulator pressure and the generated power. In this context, there are two contradictive objectives: on the one hand, constant motor torque and hence power delivery are desirable. However, this may imply a fairly fast and progressive discharging of the HP accumulator as the displacement is increased to compensate for the discharge pressure drop, possibly inducing the risk of a generator standstill. Therefore, on the other hand, maintaining the accumulator pressure as constant as possible is desirable in order to guarantee continuity of power generation, but will compromise the power level constancy. An optimum control strategy will try to achieve both objectives to a satisfactory degree by combining power and pressure control in conjunction also with the wave forecast of the top level control. In the study presented here, a proportional pressure control approach has been adopted as a first step.

V. Proof of Concept

A. Simulation Model

In order to verify the functionality of the hydraulic PTO concept, a simulation model comprising the hydrodynamic behaviour of the Wavebob wave energy device, the control system and the hydraulics of the proposed PTO concept has been developed, see Fig. 10 for a schematic of the simulation model.

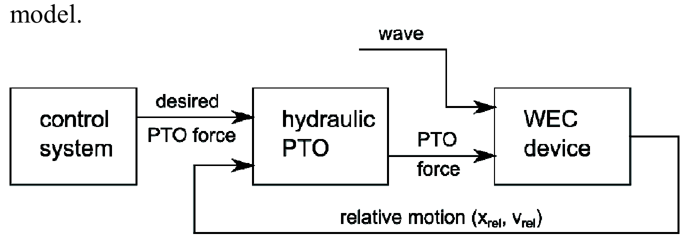

Fig. 10 Schematical block diagram of the simulation model

The mathematical modelling of the hydrodynamic behaviour of the wave energy converter is based on the heave-only time-domain model discussed in [15] and can in brief be described by the following two differential equations:

$$(m_1 + m_{11})\ddot{x}_1 + m_{12}\ddot{x}_2 + b_1\dot{x}_1 + \rho g A_{W1} x_1 = F_1 + F_{rad1} + F_{PTO} \quad (1)$$

$$(m_2 + m_{22})\ddot{x}_2 + m_{21}\ddot{x}_1 + b_2\dot{x}_2 + \rho g A_{W2} x_2 = F_2 + F_{rad2} - F_{PTO} \quad (2)$$

where x_1, x_2 are the heave displacements; m_1, m_2 are the masses; m_{11}, m_{22} are the added masses at infinite frequency, m_{12}, m_{21} are the cross terms of the added mass at infinite frequency; b_1, b_2 are a first order approximation of the viscous drag coefficients, ρ is the density of water, g the acceleration of gravity, A_{W1}, A_{W2} are the water plane areas; F_1, F_2 are the excitation forces in heave, F_{rad1}, F_{rad2} are the radiation forces and F_{PTO} is the PTO force. The subindices 1 and 2 refer to the bodies 1 and 2, respectively. Note that the radiation forces F_{rad1} and F_{rad2} are both a function of the time derivatives of x_1 and x_2 and can be calculated using convolution integrals or an equivalent linear dynamic system [19]. The PTO force F_{PTO} is a nonlinear function of the relative heave $x_{rel} = x_1 - x_2$ and its first time derivative, among others (cf. Equation 3 through 5).

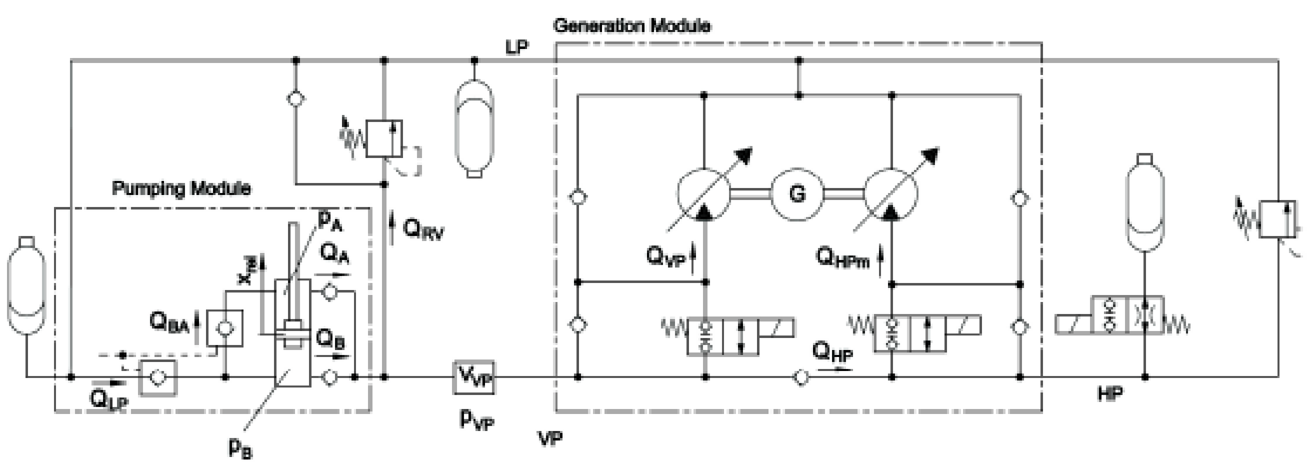

Fig. 11 Notation of the Hydraulic Parallel Circuit

The hydraulic circuit of Fig. 7 has been modelled under the following assumptions:

- No losses (no pressure drop) in the pipes and hoses
- No leakage in the hydraulic cylinders
- A lumped parameter approximation of the dynamics of the pipes and hoses is used, i.e. the pipes and hoses are modelled as a single volume.
- The check valves are modelled without dynamic effects (no inertia effects of the moving bodies), only the pressure drop is under consideration
- The accumulators are modelled with the assumption of isentropic state transitions
- The dynamics of the swash plate mechanism of the hydraulic motors has been neglected (the dynamics of the swash plate mechanism is expected to be much faster than the period of the waves)

Based on these assumptions the mathematical model of the hydraulic circuit (see [16],[17],[18] for details on modelling of hydraulic components) can be composed using the mathematical model of the hydraulic cylinders, the summarised volume of the pipes and hoses, the check valves, the LP and HP accumulators and the hydraulic motors, cf. Fig. 11. The mathematical model of the hydraulic cylinders comprises firstly the pressure build-up according to

$$\frac{dp_A}{dt} = \frac{\beta}{V_{0A} - A_1 x_{rel}} \left(Q_{BA} - Q_A + A_1 v_{rel}\right) \tag{3}$$

$$\frac{dp_B}{dt} = \frac{\beta}{V_{0B} + A_2 x_{rel}} \left(Q_{LP} - Q_{BA} - Q_B - A_2 v_{rel}\right) \tag{4}$$

with the pressures p_A and p_B, the flow rates Q_A, Q_{BA}, Q_B, the relative velocity v_{rel} and the parameters β (bulk modulus of the compressible oil), V_{0A}, V_{0B} (entrapped oil volumes including plumbing volume of sides A and B at center position $x_{rel} = 0$), A_1 and A_2 (effective piston area of sides A and B), and secondly the resulting PTO force (damping force) acting on the WEC device given by

$$F_{PTO} = p_B A_2 - p_A A_1 \,. \tag{5}$$

Correspondingly, the model of the pipes and hoses based on the aforementioned assumptions is given by

$$\frac{dp_{VP}}{dt} = \frac{\beta}{V_{VP}} \left(Q_A + Q_B - Q_{VP} - Q_{HP} - Q_{RV}\right) \tag{6}$$

with the pressure p_{VP} and the flow rates Q_{VP}, Q_{HP} and Q_{RV} (Q_{RV} is only relevant if the relief valve opens to prevent the system from overload). The flows Q_A, Q_B, Q_{BA}, Q_{VP}, Q_{HP} are governed by the mathematical model of the check valves

$$Q = \begin{cases} \dfrac{Q_n}{\sqrt{\Delta p_n}} \sqrt{\Delta p} & for\, \Delta p > 0 \\ 0 & else \end{cases} \tag{7}$$

with the pressure drop Δp (e.g. in case of check valve A with cracking pressure p_{crack}: $\Delta p = p_A - p_{VP} - p_{crack}$) and the parameters Q_n (nominal flow rate) and Δp_n (nominal pressure drop). The flow rate Q_{RV} through the relief valve can be modelled as a check valve with a cracking pressure of 300 bar.

The mathematical model of the hydraulic accumulators is given in the case of the high pressure accumulator by

$$\frac{dp_{HP}}{dt} = \frac{\kappa\, p_{HP}}{V_{accHP}} \left(Q_{HP} - Q_{HPm}\right) \tag{8}$$

and in the case of the low pressure accumulator by

$$\frac{dp_{LP}}{dt} = \frac{\kappa\, p_{LP}}{V_{accLP}} \left(Q_{VP} + Q_{HPm} + Q_{RV} - Q_{LP}\right) \tag{9}$$

with the pressure p_{HP} and gas volume V_{accHP} of the high pressure accumulator and p_{LP} and V_{accLP} of the low pressure accumulator, the gas constant κ and the HP motor flow Q_{HPm}.

Finally, the mathematical model of the hydraulic motors is given by

$$Q = \frac{1}{2\pi} n V_{d\max}\, \alpha_{rel} \tag{10}$$

with the number of revolutions n, the maximum displacement per revolution V_{dmax} and the relative displacement α_{rel}.

B. Simulation Results

The wave profile shown in Fig. 12 is an excerpt of the dominant sea state at the deployment site off the coast of Portugal. It is used as an excitation input to the following simulations. This wave profile corresponds to a sea state characterised by a significant wave height H_s of 1.75 m and a peak period T_p of 11.5 s (corresponding to a wave energy flux of approximately 17.6 kW/m). It is used to generate the excitation forces for the simulation results below. Although this sea state is the most representative one for the simulated deployment site, conclusions derived from the simulation results are not necessarily valid for the wave climate as a whole. Further simulation studies will be performed in order to provide a complete validation basis.

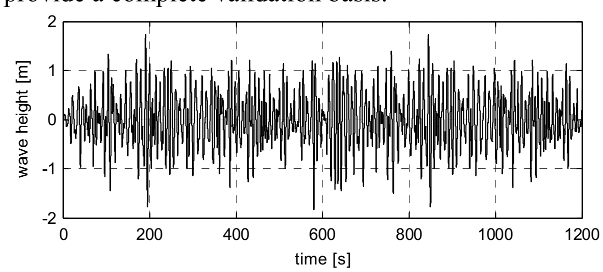

Fig. 12. Characteristic wave profile of the test site

When the Wavebob is excited by this wave profile using the aforementioned damping strategy, it reacts with a relative motion as depicted in Fig. 13. The relative position (top) includes a slight offset towards positive values. This is due to a static residual force caused by the combination of unequal area ratios of the cylinders and the size ratio of the pumping modules and is balanced by the resulting shift in buoyancy.

The instantaneous power absorbed from the waves (damping force multiplied by the relative velocity) is plotted at the top of Fig. 14, normalised to the peak wave power. The mechanical wave input is extremely irregular with a ratio of mean power to peak power of 3.4 %. At the bottom of the figure, the electrical generator output power with a mean normalised value of 2.2 % is depicted. Owing to the buffering

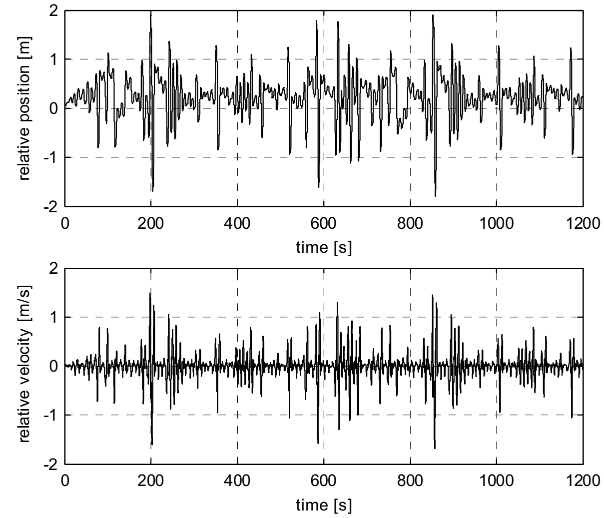

Fig. 13. Relative motion between torus and float

effect of the hydraulic accumulators, an installed power capacity of only 4.6 % of the peak input power is necessary. A direct drive PTO system would in contrast need to be rated for full peak power. These data prove the excellent smoothing performance of the hydraulic PTO circuit and the high level of utilisation of the installed power. However, the efficiencies of the hydraulic motors and the electric generator have not yet been included in the simulation model, so that the actual output power can be expected to be somewhat lower. Oncoming investigations will be looking into this.

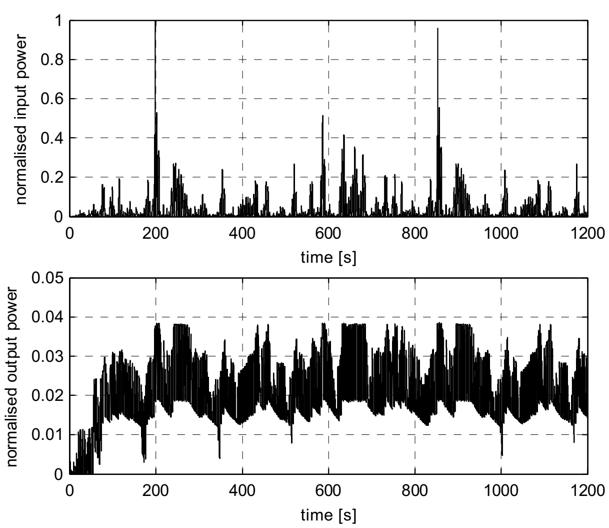

Fig. 14. Absorbed mechanical power (top) and electrical output power (bottom), normalised to the peak input power

Information on the behaviour of the hydraulic motors can be extracted from Fig. 15 through 17. As expected, the VP motor displacement is frequently ramped up and down with the relative velocity. In contrast, the HP motor is operated at nearly constant displacement near the maximum displacement during most of the simulation time. Hence, good motor efficiency can be expected. Moreover, this results in a very smooth power output of the generator.

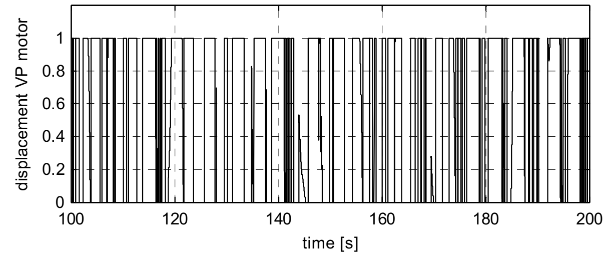

Fig. 15. Relative displacement of the VP motor (detail)

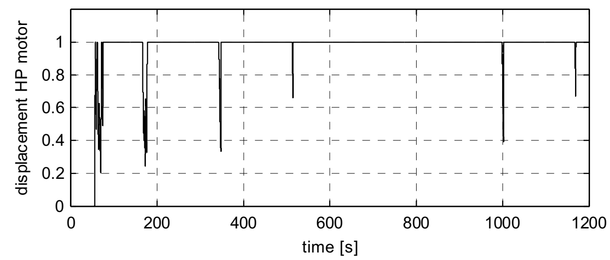

Fig. 16. Relative displacement of the HP motor

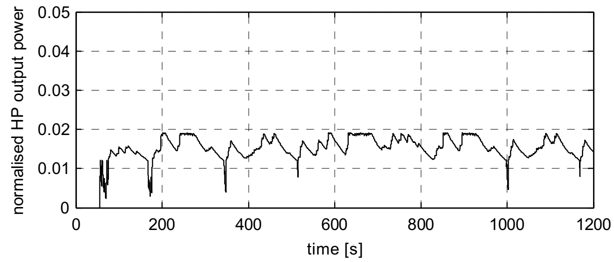

Fig. 17. Output power of the HP motor, normalised to the peak input power

Furthermore, Fig. 17 shows that the HP motor receives enough stored energy from the accumulator to sustain a fairly constant power output at a high mean level. This proves that motor and accumulator sizes are matched appropriately.

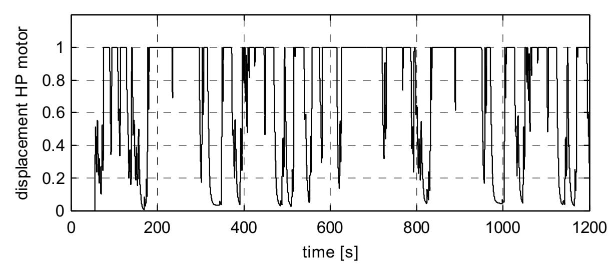

Fig. 18. Relative displacement of the double-sized HP motor

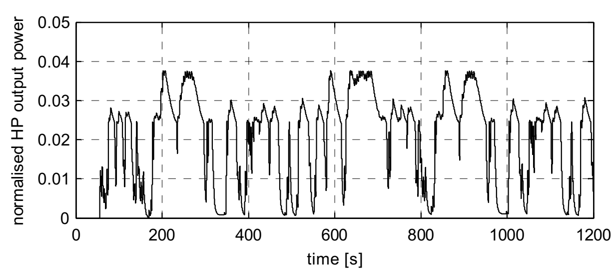

Fig. 19. Output power of the double-sized HP motor, normalised to the peak input power

The effect of suboptimal matching is demonstrated in Fig. 18 and 19. Here, the maximum motor displacement has been doubled. This results in intermittent operation characterised by frequent swashing back of the motor displacement and drops in the output power. The reason is that the accumulator size is insufficient to constantly feed the motor.

From the above elaborations can be concluded that it is necessary with regard to the overall efficiency of the hydraulic PTO system to suitably dimension the hydraulic motors and accumulators for the prevailing wave climate of the deployment site. Taking into account long-term wave measurement data, the annual energy output can thus be maximised by means of a comprehensive optimisation strategy.

CONCLUSIONS

A novel hydraulic PTO design for a heaving buoy type WEC has been presented. Two different hydraulic concepts have been analysed: one using a serial power flow path for generation (Hydraulic Transformer Circuit) and another using a parallel power flow path (Hydraulic Parallel Circuit).

The HPC is found to be the superior concept due to fewer power conversion steps, more appropriate component sizing, and parallel power conversion, resulting in better overall efficiency. The new modular failsafe design involves two pumping modules and two generator modules for increased redundancy and optimised power adaptation. Accumulators are used for energy storage and thus provide a smooth electrical power output.

A non-linear damping control approach has been tested in simulation. Numerical results for typical sea conditions have proven the effectiveness of the proposed control concept. It has been shown that even under irregular sea conditions it is possible to obtain a smooth power output from a Wavebob wave energy converter.

Upcoming future work will be focussed on extending the analysis from one sea state to an optimisation considering the full annual wave climate.

ACKNOWLEDGMENT

The research leading to these results has received funding from the European Community's Seventh Framework Programme for Research and Technological Development (FP7/2007-2013) under grant agreement n° 239376 (STANDPOINT Project). The authors also want to thank all partners of the STANDPOINT project for their fruitful contributions.

REFERENCES

[1] R. Henderson, *Design, Simulation and Testing of a novel hydraulic power take-off system for the Pelamis wave energy converter*, Renewable Energy, vol. 31, issue 2., pp. 271-283, Feb. 2006.

[2] C. Signorelli, C. Villegas and J. Ringwood, *Hardware-In-The-Loop Simulation of a Heaving Wave Energy Converter,* 9th European Wave and Tidal Energy Conference, 2011. [Under review]

[3] M. Livingstone and A. Plummer, "The Design, Simulation and Control of a Wave Energy Converter Power Take Off", in *Proc. 7th International Fluid Power Conference*, p. 1-13, 2010.

[4] H. Polinder, M.E.C. Damen and F. Gardner, *Design, modelling and test results of the AWS PM linear generator",* European Transactions on Electrical Power, vol. 15, pp. 245-256, 2005.

[5] R. Waters, *Energy from Ocean Waves-Full Scale Experimental Verification of a Wave Energy Converter,* PhD dissertation, Uppsala University, 2008.

[6] M. Blanco, M. Lafoz, G. Pinilla, L. Gavela, L. García-Tabarés and A.Echeandia, *Electric Linear Generator to Optimize Point Absorber Wave Energy Converter,* In proc. Of 3rd International Conference on Ocean Energy (ICOE), Bilbao, 2010.

[7] S.H. Salter, J.R.M. Taylor and N.J. Caldwell, *Power conversion mechanisms for wave energy*, Proc. Of the Institution of Mechanical Engineers, Part M: Journal of Engineering for the Maritime Environment, vol. 216, issue 1, 2002.

[8] A. F. de O. Falcão, *Modelling and control of oscillating-body wave energy converters with hydraulic power take-off and gas accumulator,* Ocean Engineering, vol. 34, pp 2021-2032, 2007.

[9] N. Rousseau, M. Rosa-Clot and F. Danos, *Report on the state of ocean energy in Europe: technologies, test sites, and joint projects*, EquiMar Deliverable D9.1, 2010, Available: https://www.wiki.ed.ac.uk/download/attachments/9142387/Equimar+D+9.1+EU-OEA-2.pdf?version=1.

[10] F. Fusco and J. Ringwood, *Short-Term Wave Forecasting for Real-Time Control of Wave Energy Converters,* vol. 1, issue 2, pp. 99-106, 2010.

[11] A. Babarit, M. Guglielmi and A.H. Clément, *Declutching control of a wave energy converter*, Ocean Engineering, vol. 36, pp. 1015-1024, 2009.

[12] H. Eidsmoen, *Optimum Control of a Floating Wave-Energy Converter With Restricted Amplitude,* Journal of Offshore Mechanics and Arctic Engineering, vol. 118, issue 2, pp. 96-102, 1996.

[13] A. Falcão, P. Justino, J. Henriques, J. André*, Reactive versus Latching Phase Control of a Two-body Heaving Wave Energy Converter*, In Proc. Of the European Control Conference ECC'09, Budapest, Hungary, 2009.

[14] A. Barbarit, A. Clement, Optimal latching control of a wave energy device in regular and irregular waves, Applied Ocean Research, vol. 28, pp. 77-91, 2006.

[15] J. J. Cândido, and J. A. P. Justino, "Frequency, stochastic and time domain models for an articulated wave power device", *Proceedings of the ASME 27th International Conference on Offshore Mechanics and Arctic Engineering (OMAE2008)*, paper OMAE2008-57253, pp. 633-643, 2008.

[16] J.F. Blackburn, G. Reethof, J.L Shearer, *Fluid Power Control,* John Wiley & Sons, New York, 1960.

[17] D. McCloy, H.R. Martin, *Control of Fluid Power: Analysis and Design* (2nd Edition), John Wiley & Sons, New York, 1967.

[18] H.E. Merrit*, Hydraulic Control Systems*, John Wiley & Sons, New York, 1967.

[19] G. Duclos, A. H. Clément, and G. Chatry "Absorption of outgoing waves in a numerical wave tank using a self-adaptive boundary condition", *International Journal of Offshore and Polar Engineering*, Vol. 11, No. 2, pp. 104-111, Jun 2001.

Implementation of a Pitch Stability Control for a Wave Energy Converter

Carlos Villegas*, Haite van der Schaaf†
*Wavebob Limited
Maynooth, Ireland
E-mail: Carlos.Villegas@wavebob.com
†Maritime Research Institute Netherlands
Haagsteeg 2 / P.O. Box 28
6700 AA Wageningen, The Netherlands
E-mail: H.v.d.Schaaf@marin.nl

***Abstract*—A point absorber wave energy converter relies mainly on heave motion to convert energy from the ocean waves into electrical power. However, heave motion can be affected by the high pitch and roll motions resulting from parametric resonance. It is well known that floating structures can be subject to parametric instability arising from variations of the pitch restoring coefficient. Insights into such instability can be obtained by making Mathieu equation-like approximations. In particular, it is known that the instability is due to harmonic variations at half the pitch resonance period of the floating structure. Several approaches have been considered in the literature to deal with parametric resonance. In this paper, we use the power take-off of a wave energy converter to reduce parametric resonance. Experimental results in a wave basin validate the approach.**

***Index Terms*—wave energy, point absorber, pitch control, PTO emulation, parametric resonance, mathieu stability.**

I. Introduction

The technical challenges involved in the conversion of ocean wave energy into useful electrical power are substantial. There is a perceptible convergence towards floating, offshore systems that are adapted to respond in accordance with the incident wave climate and thus maximize energy absorption. The available energy in the oscillating system may be transformed, via a power take-off (PTO), to useful electrical power. The interaction between the oscillating bodies and the PTO is therefore of vital importance to the optimization of energy conversion. In particular, large pitch motion in a heaving buoy wave energy converter may affect the available useful power at the PTO.

The main source of large pitch motions can be associated with parametric resonance. Parametric resonance has been widely investigated for ships [1] and offshore platforms [2] and has been analyzed using various non-linear approaches such as describing functions, the circle criterion or the extended Popov criterion. Such behavior for a heaving buoy wave energy converter arises from harmonic variations in the pitch restoring coefficient caused by large heaving motions close to twice the pitch resonance frequency. While there are various approaches to deal with the parametric resonance of floating structures - such as using heave damping [3], shape adjustments [4] and specific mooring designs [2] - an adaptive approach to cancel parametric resonance would allow for more design flexibility.

In this paper, we investigate the use of a controlled PTO system to avoid parametric resonance of a wave energy converter using the concept of Harmonic balance. Following a non-linear analysis of the equations of motion of a heaving buoy wave energy converter, we develop a control strategy to cancel such instabilities. In order to implement such control system in a wave tank, a controlled linear actuator was fitted between the two oscillating bodies to emulate the dynamics of a full-scale PTO system. Details of the implementation and testing of such equipment are also described. Simulation and experimental results from tank tests at the Maritime Research Institute Netherlands (MARIN) are presented to validate the effectiveness of the pitch stability control to cancel parametric resonance while increasing power capture.

II. A Primer on instability on the Mathieu Equation

Instability mechanisms in the Mathieu equation are well undestood. For a good discussion see [5] and [6]. For completeness, we now give a very brief discussion of the instability mechanism here. We consider the following equation:

$$\ddot{y} + \zeta\dot{y} + (a - bcos(\omega t))y = 0. \tag{1}$$

Ignoring some important mathematical details concerning the existence of transforms, this equation may be written (roughly speaking) using Laplace transforms as:

$$Y(s) = \frac{0.5b}{s^2 + \zeta s + a}\big(Y(s - j\omega) + Y(s + j\omega)\big) \tag{2}$$

Once the equation is in this form one may apply Harmonic balance arguments to postulate the existence of periodic motion to characterize the boundary of instability. Note that the effect of the cosine is to split the feedback signal into two sidebands. Using Harmonic balance arguments, the condition for instability is that some frequency has a unity amplification and a phase shift of 2π in the feedback loop. By assuming that one of the sidebands is filtered out as a result of low-pass filter characteristics, and by using standard Harmonic balance arguments (akin to Describing function analysis), one readily concludes (approximately) that this may be achieved for any modulation frequency that is twice the frequency at which the bode plot of $\frac{b}{2}G(s)$, $G(s) = 1/(s^2+\zeta s+a)$, has an magnitude amplification greater or equal to one. Details of this argument are given in [6] and are written rigorously in [7]. Before proceeding some comments are merited.

(i) This is an argument based on Harmonic balance. It is identical in spirit to Describing function analysis and can be justified on this basis.

(ii) The technique can be applied to any periodic multiplier by replacing it with its Fourier series.

(iii) The analysis clearly identifies the importance of the resonance frequencies of $G(s)$ and identifies mechanisms that excite these modes using a time-varying multiplier. Our idea in this paper is to avoid exciting these dangerous frequencies using a notch filter (perhaps adaptively).

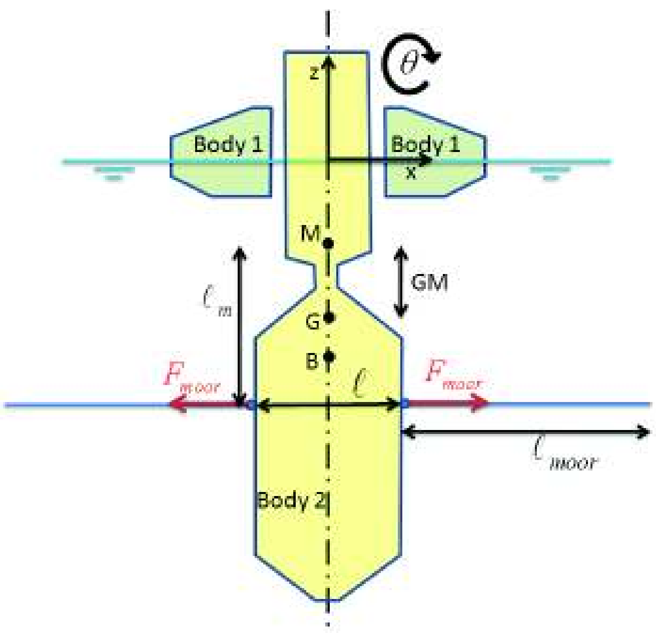

Fig. 1. Graphical representation of a wave energy converter

A. Modelling of a wave energy converter

Consider the simplified heave and pitch equations of motion of a heaving buoy composed of two bodies as depicted in Fig. 1:

$$\begin{aligned}(m_1+m_{11})\ddot{z}_1 + m_{12}\ddot{z}_2 + b_1\dot{z}_1 + \rho g A_1 z_1 \\ = F_1 + F_{rad1} + F_{PTO}\end{aligned} \tag{3}$$

$$\begin{aligned}(m_2+m_{22})\ddot{z}_2 + m_{21}\ddot{z}_1 + b_2\dot{z}_2 + \\ \left(\rho g A_2 + \frac{2F_{moor}}{\ell_{moor}}\right) z_2 = F_2 + F_{rad2} - F_{PTO}\end{aligned} \tag{4}$$

$$\begin{aligned}(J+J_\infty)\ddot{\theta} + b_\theta\dot{\theta} + \left(k_\theta + F_{moor}\ell + 2k_{moor}\ell_m^2\right)\theta \\ = F_\theta + F_{rad\theta}\end{aligned} \tag{5}$$

TABLE I
NOTATION OF MODEL

Symbol	Description
η	Wave elevation $[m]$
θ	Pitch angle [degrees]
z_i	Heave motion of i-th body $[m]$
m_i	Mass of i-th body $[kg]$
J	Mass moment of inertia $[kgm^2]$
J_∞	Infinite added inertia $[kgm^2]$
m_{ij}	Infinite added mass of i-th body relative to j-th body $[kg]$
ρ	Density of water $[kg/m^3]$
g	Acceleration of gravity $[m/s^2]$
GM	Metacentric height $[m]$
∇	Submerged volume $[m^3]$
ℓ	Distance between mooring connecting points $[m]$
F_{moor}	Pretension mooring force $[N]$
b_i	Damping in heave for i-th body $[Ns/m]$
b_θ	Damping in pitch $[Nms]$
A_i	Waterplane area of i-th body $[m^2]$
F_i	Excitation force in heave for i-th body $[N]$
$F\theta$	Excitation moment in pitch $[Nm]$
F_{radi}	Radiation force in heave for i-th body $[N]$
$F_{rad\theta}$	Radiation moment in pitch $[Nm]$
F_{PTO}	PTO force $[N]$
k_{moor}	Mooring stiffness $[N/m]$
ℓ_{moor}	Length of horizontal mooring line $[m]$
ℓ_m	Vertical distance from M to mooring connecting point $[m]$
G	Centre of gravity
B	Centre of buoyancy
M	Metacentre

where k_θ is the time-varying pitch restoring coefficient. Refer to Table I for a description of the notation used. The restoring coefficient can be represented as a function of the displaced volume and the steady-state metacentric height [2]:

$$k_\theta = \rho g \nabla GM, \tag{6}$$

but once there is heave motion of the wave energy converter and a wave elevation, both the volume and the metacentric height change approximately by:

$$GM_{new} = GM - 0.5(\tilde{z} - \eta) \tag{7}$$

$$\nabla_{new} = \nabla - A_1(z_1-\eta) - A_2(z_2-\eta) \tag{8}$$

where:

$$\tilde{z} = \frac{A_1 z_1 + A_2 z_2}{A_1 + A_2} \tag{9}$$

The new restoring coefficient k_θ can be written as:

$$\begin{aligned}k_\theta = \rho g \nabla GM - 0.5\rho g\left(\nabla + 2GM(A_1+A_2)\right)(\tilde{z}-\eta) \\ +0.5\rho g(A_1+A_2)(\tilde{z}-\eta)^2\end{aligned} \tag{10}$$

In order to illustrate the effect of the PTO force on the heave motion of the two bodies (z_1,z_2), consider a typical PTO force defined as $F_{PTO} = -D(\dot{z}_1 - \dot{z}_2)$ where D is a damping coefficient. The PTO force is the force linking the two bodies. The frequency response of the two bodies to a wave (transfer function ampitude) is depicted in Fig. 2. The damping value (D) clearly affects the vertical response of the bodies by moving the two eigenvalues of the system close together as damping increases. Note that when the body is locked, *i.e.* $D = \infty$, the two eigenvalues are equal.

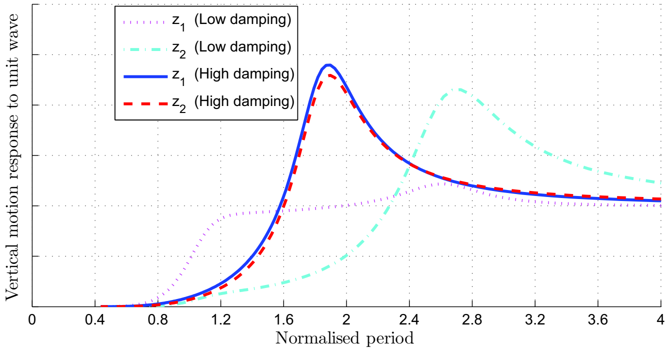

Fig. 2. Transfer function of vertical motion to wave amplitude for a high damping coefficient and a low damping coefficient.

B. Parametric resonance of a wave energy converter

The importance of the Mathieu system in analysing floating devices has already been postulated; see [2]. However, waves are not really periodic, and they are certainly not cosines. But they are almost periodic, and given that the Mathieu analysis can be extended to general periodic multipliers, the study of this equation gives insights that can be used for control design. In particular, the Mathieu analysis shows that periodic multipliers that have significant frequency components at twice the resonant frequency of the pitch dynamics are most dangerous. In this paper we give a simple control design that is based on reducing the loop gain at this frequency. In particular, propose an approach to reduce the harmonic excitations at half the resonance period by using the PTO force. In the next section, we present an experimental validation of the approach leading to a reduced pitch motion and increased power capture of the wave energy converter.

First of all note that in this simplified model there is coupling from Equations 3 and 4 to Equation 5 but not in the other direction. Furthermore, note that the inputs to Equations 3 and 4 are a function of the wave elevation that we assume to be a combination of sinusoids. Thus, since Equations 3 and 4 are both linear ordinary differential equations, and based on experimental observations we assume that in steady-state the outputs z_1 and z_2 are both combinations of sinusoids. Notice that this assumption is consistent with simulations and experimental observations.

For the analysis, let us consider that the variations of the pitch restoring coefficient are mainly affected by the variations of GM from Equation 7. Also, as we aim to affect parametric stability using the PTO forces, let us also ignore the wave elevation effect. As a result, the variations in the pitch restoring coefficient are a function of $\tilde{z}$ [2]:

$$k_\theta = \rho g \nabla (GM - 0.5\tilde{z}) \tag{11}$$

If we assume a sinusoidal wave affecting the wave energy converter at a frequency ω, that the input from the waves restoring coefficient k_θ can be rewritten as a one term harmonic [2] and the pitch equation of motion in Equation 5 can be approximated as a Mathieu equation:

$$\ddot{\theta} + \xi\dot{\theta} + (a - bcos(\omega t + \phi_c))\theta = u \tag{12}$$

where ϕ_c is the phase angle of $\tilde{z}$ at that frequency and:

$$\xi = \frac{b_\theta}{J + J_\infty}, a = \frac{\rho g \nabla GM + F_{moor}\ell + 2k_{moor}\ell_m^2}{J + J_\infty},$$
$$b = \frac{\rho g \nabla |\tilde{z}|}{2(J + J_\infty)} \text{ and } u = \frac{F_\theta + F_{rad\theta}}{J + J_\infty}.$$

It is well known that the the Mathieu equation (see Equation 12) could be subject to parametric instability for harmonic excitations around half the resonance period of the linear time-invariant system $G(s) = 1/(s^2 + \xi s + a)$. The amplitude of $G(s)$ is plotted as a function of frequency in Fig. 3.

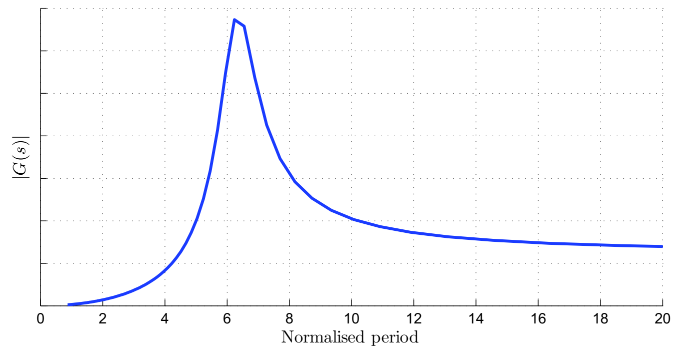

Fig. 3. Transfer function amplitude of $G(s)$.

III. Experimental Results

It was confirmed in simulation that by reducing the amplitude of $\tilde{z}$ for periods close to half the resonance frequency of pitch, the parametric resonance could be practically removed. In particular, a notch filter applied to the PTO force at half the resonance frequency of pitch reduced the parametric resonance of the wave energy converter. This approach was tested in the MARIN wave basin in Netherlands using a small scale wave energy converter (see Fig. 4). In this section, we present a brief description of the PTO used for the scaled model followed by experimental results for the control approach.

A. Linear actuator as PTO system

One of the major tasks for scale-model testing of the wave energy converter is the design of an accurate PTO system. The main function of this scale-model PTO is to track a desired force between the two bodies based on various control algorithms. The available mechanical energy for conversion into electricity can be determined from the available force and relative speed sensors.

For the tests of the pitch controller, a linear motor was used as a PTO for the scale model. Such a linear motor satisfied the main velocity, force and stroke PTO requirements. Alternatively, a rotating PTO could have been used as in [8]. In this case, a Copley Controls linear motor system was used consisting of a housing with windings (stator) and a moving rod with magnets (translator). The force between the

Fig. 4. Wave tank tests device in MARIN's Seakeeping basin.

bodies was measured using a 6 degree of freedom (DoF) force frame, the position was measured using an accurate position transducer in the motor housing and an acceleration sensor was fixed on body 2. The complete setup is shown in Fig. 5. The red parts are moving with body 1 and the blue parts are fixed to body 2. The six component frame (including the 6 DoF force sensor) is mounted in body 2 and measures the total mechanical force between the two bodies.

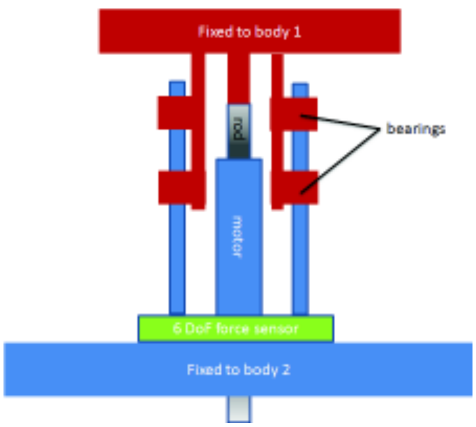

Fig. 5. System setup for PTO using linear actuator.

The linear motor was controlled in current mode using a servo amplifier. In this mode, the force is proportional to the applied electric current. This force is generated inside the motor and will not be equal to the force acting between the bodies since force is lost due to bearing friction and Eddy effects. By using a feedback system of the measured force, the linear motor control could compensate for such losses. The force between the two bodies was obtained using the six component frame (6DoF force sensor) with a correction taking the acceleration of the frame mass into account.

MATLAB Simulink was used to determine a suited controller structure. The very small time constant of the drive/motor (typically 3 ms, 1st order response) in combination with limited digital controller update rates (500Hz) could easily lead to instability. To prevent such instabilities, we found that using only an integral control gain, the tracking response is improved as well as the closed-loop bandwidth. The linear motor was mounted in a test-rig to validate the force control design. In Fig. 6, the force tracking step response of the linear motor using a controller with an integral gain is presented.

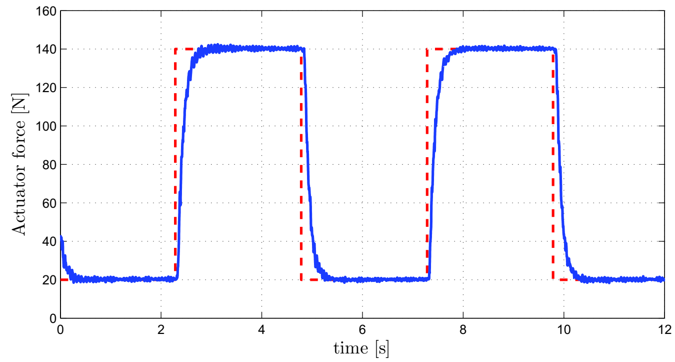

Fig. 6. Closed loop step response of linear motor in a test-rig. The reference force (dashed) is tracked by the measured force (solid).

To speed up the system response, it can be beneficial to compensate beforehand for known friction losses using in this case feedforward control. The feedforward control implemented dealt with viscous friction losses and stiction. The total setup consisting of integral control and feedforward terms is shown in Fig. 7.

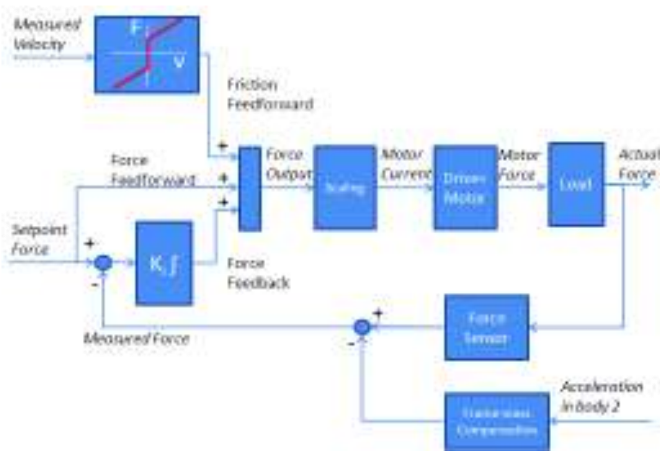

Fig. 7. Diagram of the force tracking control for the linear motor.

After testing the linear motor and its controller in the test-rig, they were installed in the wave energy converter. By using the 6 DoF force sensor and the vertical acceleration of the body 2, it is possible to obtain the connecting force between body 1 and body 2. Such force, referred to as Measured Force in Fig. 7, includes both the force of the linear motor and the bearings. The effectiveness of the force tracking using the friction feedforward control is depicted in Fig. 8 for a

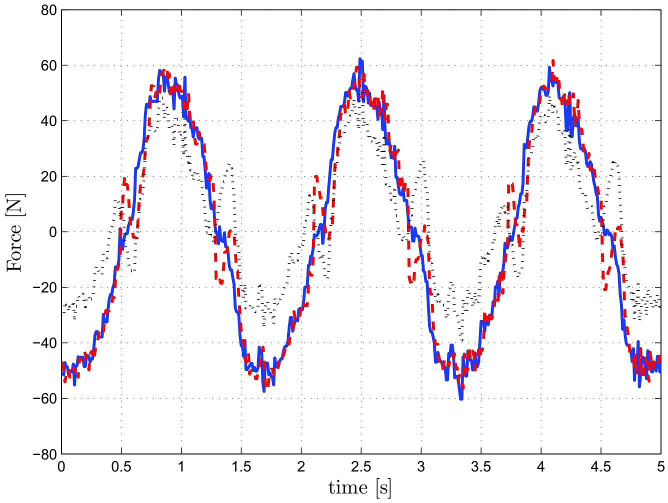

Fig. 8. Force tracking of linear motor installed in wave energy converter. Force Output (solid), Measured Force (dashed) and Force Output (dotted).

monochromatic wave in the wave basin. Note that the Setpoint force is the desired PTO force F_{PTO}. In this case, the Setpoint Force or PTO force (solid) is simply a damping force, *i.e.* proportional to the velocity measurement. The Measured Force (dashed) is able to track the desired Setpoint Force (solid) with practically no effect of friction except at the zero crossing. Notice that the Force Output signal (dotted) going to the linear motor has an offset with respect to the Measured Force as the remaining force is provided by friction. As a result, the actual force required by the linear motor is smaller than the required total force from the Setpoint Force in the case of damping forces.

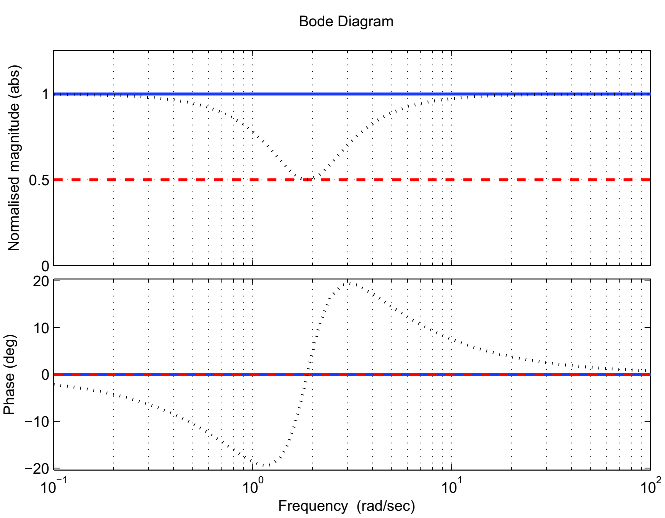

Fig. 9. Bode plots for the high damping (solid), low damping (dashed) and the high damping with notch filter (dotted).

B. Experimental results

In the wave tank, the wave energy converter was subject to waves representative of the same North Atlantic sea conditions during three different tests (see Fig. 10(a)). Initially, linear simulations suggested to use a high damping to optimize power capture, that is, to use $F_{PTO} = -D(\dot{z}_1 - \dot{z}_2)$. However, experimental tests with such damping resulted in higher than expected pitch and much lower mechanical power capture (see Fig. 10(b) and 10(c)). To remove parametric resonance, we considered both reducing the overall PTO damping D or applying a notch filter at half the resonance period to the reference PTO force. The notch filter used was multiplied by the high damping constant, that is:

$$F_{PTO}(s) = -DN(s)Z_{rel}(s) \tag{13}$$

where $N(s)$ is the notch filter transfer function; and $F_{PTO}(s)$ and $Z_{rel}(s)$ are the Laplace transforms of F_{PTO} and $\dot{z}_1 - \dot{z}_2$, respectively. The bode plots of the damping constants and the notch filter are depicted in Fig. 9.

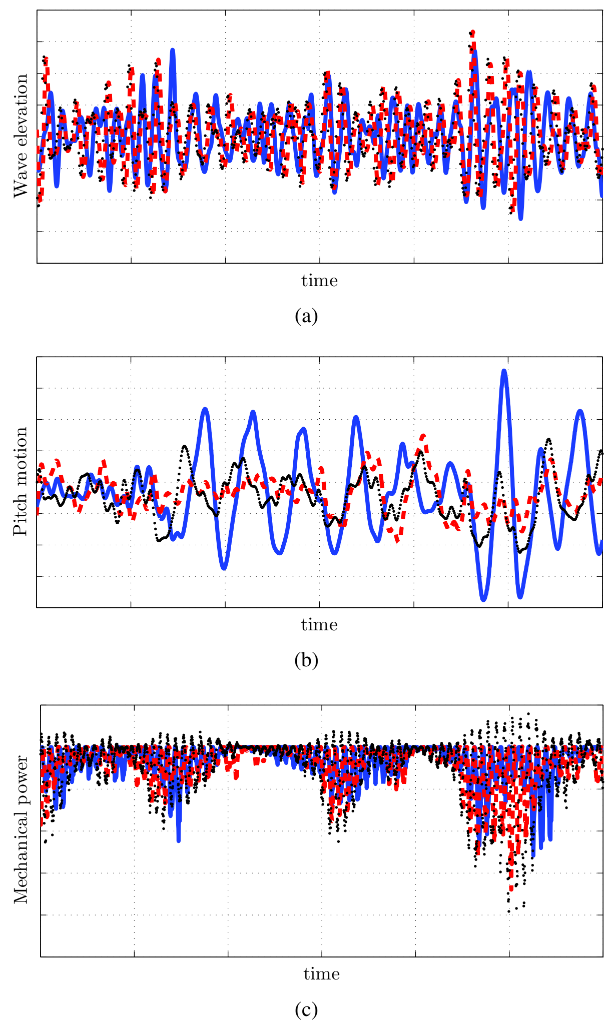

Fig. 10. (a) Wave elevation, (b) pitch motions and (c) mechanical power for experimental results with typical north sea wave conditions for high damping at the PTO (solid), low damping (dashed) and high damping with a notch filter (dotted).

Reducing the damping and the notch filter reduced pitch motion and increased power capture. Specifically, for the Atlantic sea conditions tested at the wave basin, reducing pitch motion led to an increase of 25% of the mean mechanical power captured. Notice that some motoring power was required by the PTO for the specific notch filter used (see Fig. 10(c)). In spite of such instantaneous motoring power, the mean power captured by the wave energy converter increased by 25%. Finally, in order to operate for different sea states without affecting power capture, the proposed pitch controller would require an adaptive strategy depending on the current sea conditions. As a result, detection of the sea conditions using methods such as wave forecasting would lead to an adaptive filter to deal with parametric resonance.

IV. Conclusion

In this paper we present a control approach to reduce parametric resonance of a wave energy converter. By using insights from the Mathieu equation, it was found that by applying a notch filter at half the resonance period to the PTO force it was possible to reduce parametric instability. Experimental results were carried out in a wave basin using a linear motor with a force tracking controller as PTO. The results demonstrated the approach to reduce parametric resonance with such notch filter leading to lower pitch motions and higher mechanical power output. For the tested Atlantic sea conditions, the mean power output of the wave energy converter was increased by 25% by using such notch filter. In this paper we ignored the direct effect of the waves on parametric resonance and future work will deal with wave amplitudes to avoid exciting the dangerous frequencies, *i.e.* resonance frequencies of $G(s)$.

Acknowledgment

This work was partly supported by the EU STANDPOINT project and by the SEAI grant number OC/OC/10/19795706. The first author (CV) gratefully acknowledges consultations with Robert Shorten of the Hamilton Institute on Mathieu Instability. Robert Shorten's time on this work was funded by SFI grant number 07/IN.1/I901. The second author (HvdS) gratefully acknowledges MARIN for funding the development and prototyping tests of the force controlled model scale PTO system.

References

[1] M. A. Neves and C. A. Rodriguez, "On unstable ship motions resulting from strong non-linear coupling," *Ocean Engineering*, vol. 33, no. 14-15, pp. 1853–1883, 2006.

[2] B. Koo, M. Kim, and R. Randall, "Mathieu instability of a spar platform with mooring and risers," *Ocean Engineering*, vol. 31, no. 2, pp. 249–256, 2006.

[3] J. B. Rho and H. S. Choi, "Heave and Pitch Motions of a Spar Platform with Damping Plate," in *Proc. of the International Offshore and Polar Engineering Conference*, Japan, May 2002.

[4] P. H. Kristensen, I. Husem, and E. Pettersen, "PLATFORM STRUCTURE, US Patent Pub. No. 2004/0040487 A1," Mar 2004.

[5] H. Power and A. Tsoi, "Improving the predictions of the circle criterion by combining quadratic forms," *Automatic Control, IEEE Transactions on*, vol. 18, no. 1, pp. 65–67, 1973.

[6] R. N. Shorten, "A study of hybrid dynamical systems with application to automotive control," Ph.D. dissertation, Department of Electrical and Electronic Engineering, University College Dublin, Republic of Ireland, 1996.

[7] K. Wulff, "Quadratic and non-quadratic stability criteria for switched linear systems," Ph.D. dissertation, Hamilton Institute, NUI Maynooth, Republic of Ireland, 2005.

[8] B. Buchner, H. v. d. Schaaf, and K. Hoefakker, "Pilot model tests on the 'green water concept' for wave energy conversion with model scale power take-ff (pto) modelling," in *OMAE2010-20484, International Conference on Ocean, Offshore and Arctic Engineering*, China, 2010.